

Development of a Test Method to Evaluate Lithium-Ion Batteries for Second Life in Renewable Energy Applications

Mussab Najeeb

*Department of Electrical Engineering
and Information Technology
Technical University of Ilmenau
Ilmenau, Germany
mussab.najeeb@gmx.de*

Prof. Dr. Ulf Schwalbe

*Department of Electrical Engineering
and Information Technology
University of
Applied Sciences Fulda
Fulda, Germany
ulf.schwalbe@et.hs-fulda.de*

Abstract— Lithium-ion batteries can still be used in many applications after removal from their first use in electric vehicles, e.g. as a storage media in photovoltaic systems and for grid support. Therefore, there is a great need to develop reliable methodologies and tools to characterize the expected performance of lithium-ion batteries after their first life in electric vehicles to enable the economical and sustainable re-use of the large amount of lithium-ion batteries, which will be available in the near future. In this paper, we will develop a robust, fast, and non-destructive measurement procedure using artificial intelligence to estimate their state of health.

Keywords— *Lithium-ion batteries, Second life of batteries, Battery modelling, Artificial neural networks, State of charge, State of health, Electrical vehicle, Energy storage systems*

I. INTRODUCTION

Due to the increase in the use of electric vehicles (EVs) in the past few years and the expected shift of the automotive market in the near future towards EVs. It is certain that the market will have large amounts of lithium-ion batteries (LIBs) that are no longer fit for use in EVs, but may represent a viable solution to the problem of high cost of batteries in energy storage systems (ESS). The re-use of LIBs in various applications and putting them into service as a second life requires a reliable measurement and testing system in order to achieve the optimal efficiency of the re-use.

In addition to cell temperature and voltage, the two most important parameters for Li-ion batteries are [1]:

- State of charge (SoC)

The state of charge is the percentage of charge available in the battery, 100% indicating full capacity

and 0% indicating that no more charge is left in the battery. The SoC parameter is very important to monitor the battery capacity level.

- State of health (SoH)

State of health indicates the amount of charge the battery can store. When a battery is new, the SoH should be close to the manufactured specification, i.e. SoH=100% but as the battery ages the SoH will start to drop. For example, a 100 Ah battery that is only able to produce 50 Ah is deemed to have 50% SoH, and it can still be charged to a SoC=100% tacking into account that the amount of charge that the battery can store being reduced.

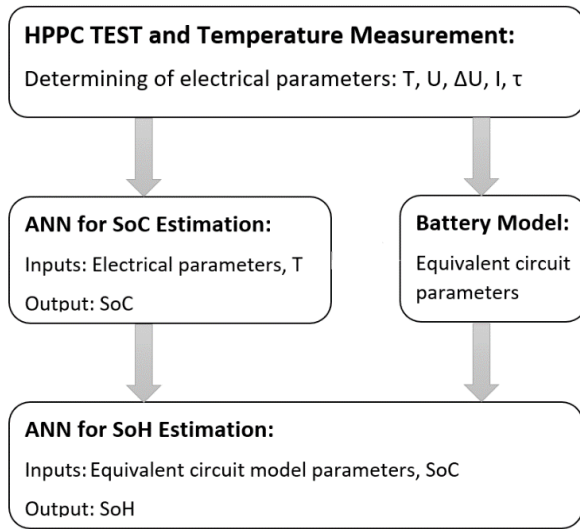
It is assumed that EV battery packs have reached the end of life when the SoH falls below 70% to 80%, at this level of SoH become the battery pack no longer fit for EVs due to the reduction in the power level, which means the battery, be either recycled or repurposed for other applications [1].

As the need for stationary energy storage systems (SESS) increases, the rapid proliferation of electric vehicles creates a fleet of millions of lithium-ion batteries that after a few years of operation are deemed unsuitable for the rigorous transportation operating cycle/environment. Because EV owners are expected to replace their battery system as soon as they have lost 20% of their capacity, these used batteries offer a tremendous opportunity to be used in new applications where the duty cycle and amperage are less burdensome than EVs. They may provide an inexpensive source of LIBs for new applications as SESS, extend the life of a battery and defer the eventual costs of recycling [2].

II. METHOD SUMMARY

This paper presents an advanced procedure for estimating the battery states (SoC and SoH) based on the artificial neural network (ANN) technology. This procedure is fast, reliable, non-destructive and accurate as described in next sections.

As shown in Fig. 1, the procedure is divided into four blocks. In the first stage, the electrical parameters are derived by applying the hybrid pulse power characterization (HPPC) and temperature (T) is measured. These parameters and T provide a good assessment of the effective capacity and SoC of the battery and this will be the task of the second stage of



the improved procedure. At this stage, measured electric parameters are entered with T to a neural network to evaluate SoC. The parameters of the equivalent circuit model (ECM) will be derived in third stage as described in our previous research (Developing an advanced equivalent circuit model for LIBs for battery monitoring purpose) [3]. Finally, in the fourth stage, SoH is estimated through the second neural network, which has all of parameters of the internal model and SoC as inputs.

Fig. 1. Block diagram of improved test method

All stages will be explained in detail in the following sections.

III. BATTERY MODELLING

A. Background:

The modelling of LIBs is very important for state monitoring. Modelling methods are classified generally into three categories: white-box, black-box, and grey-box modelling [4].

White-box models require a thorough knowledge of the internal cells' characteristics and the interactions within them. In this type of modelling, all reactions in the cell

are considered during all operational work situations (charging, discharging and standby) and under all conditions depending on the required accuracy. However, obtaining a robust and accurate model with improved system-wide performance in this way remains critical, therefore this method cannot be recommended for upgrading the model from single-scale cells to larger modules or to a LIBP, unless many simplifications are taken in Consideration [4][5].

On the contrary, black-box technologies provide practical simplification, which is why they are so widely adopted. These models are done using some techniques like support vector regression, artificial neural networks, and fuzzy logic. However, the model's ability to predict the state of the battery remains limited when any of the operational parameters are drifting outside the model's training field, because there is insufficient knowledge of the battery characteristics and the reasons for this drift [5][6].

The grey-box models were presented as a compromise between black and white-box models. The equivalent circuit model is one example of a grey-box technique [6].

Table 1 presents briefly a comparison of the three types of models [7][8].

TABLE I. COMPARISON OF THE THREE TYPES OF MODELS [7][8]

Feature	Model Types		
	White Box	Grey Box	Black Box
Base/Needs	Deterministic equations	Prior knowledge	Data driven
	Physical knowledge	Unknown parameters estimated from empirical data or literature	Inputs-Outputs representation
	Internal dynamics		
Complexity	Very high	Medium	Medium
Accuracy	High	Medium	Low-Medium
Applications	Battery design	Battery management/ monitoring	Offline analysis

B. Second-order equivalent circuit model:

As shown in Table 1, the most suitable type for the purposes of our paper is the grey box model, and the RC-equivalent circuit model is the most important form of this model. Where this type has an acceptable accuracy and do not need a deep physical knowledge or internal electrochemical analysis. This is one of the main advantages of this model, that it shifts work from a complex and dynamic electrochemical field to a relatively simple electric field.

In this paper, a second-order equivalent circuit model of battery cells is considered as describe in our previous paper and shown in Fig. 2 [3].

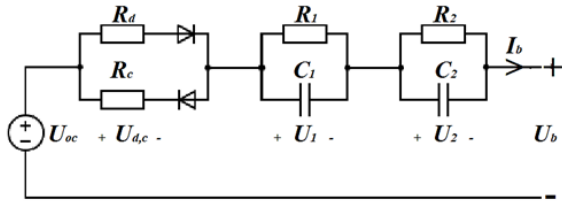


Fig. 2. Second-order equivalent circuit model

This model consists of three components: an open circuit voltage (U_{oc}), a series charge/discharge resistance (R_c/R_d), two parallel RC networks connected in series (R_1-C_1 and R_2-C_2), and two Ideal diodes (do not have a threshold voltage. The internal resistance would be zero when any forward voltage is applied across their terminals, and don't have a breakdown voltage) to connect the appropriate resistance depending on the operational condition of the battery (charging/ discharging) [9][10][11][12].

C. Model parameters identification:

According to the Kirchoff's laws, we can describe the relationships among capacitors, voltage, battery voltage (U_b), and battery current (I_b) mathematically as follows [9][10]:

$$\dot{U}_1 = \frac{I_b}{C_1} - \frac{U_1}{R_1 C_1}$$

$$\dot{U}_2 = \frac{I_b}{C_2} - \frac{U_2}{R_2 C_2}$$

$$U_b = U_{oc} - U_1 - U_2 - I_b R_{c,d}$$

For calculation we need to apply a charging and discharging pulses. Fig. 3 shows a brief illustration of the HPPC test profile, where applying period of charge/discharge pulses is 10 sec and relaxation period is 40 sec.

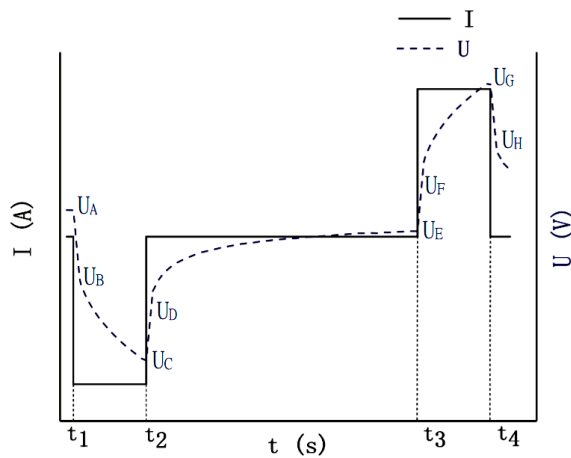


Fig. 3. Illustration of the HPPC test profile for parameters calculation

R_c , R_d , and U_{oc} under charging and discharging are determined as follows [10][11][12]:

$$R_d = \frac{U_A - U_B}{|I_b|} \tag{4}$$

$$R_c = \frac{U_F - U_E}{|I_b|} \tag{5}$$

The battery voltage during the relaxation period $U_b(t)$ while charging/discharging can be fitted to the exponential function form expressed as [10][11][12]:

$$U_b(t) = U_{oc} - R_1 I_b e^{-\frac{t}{\tau_1}} - R_2 I_b e^{-\frac{t}{\tau_2}} - I_b R_{c,d} = P_0 - P_1 e^{-k_1 t} - P_2 e^{-k_2 t} \tag{6}$$

After determining P_0 , P_1 , P_2 , k_1 , and k_2 experimentally, other model parameters could be determined in additional to (4), (5) as follows [10][11][12]:

$$\left\{ \begin{array}{l} R_1 = \frac{|P_1|}{|I_b|}; R_2 = \frac{|P_2|}{|I_b|} \\ C_1 = \frac{1}{R_1 k_1}; C_2 = \frac{1}{R_2 k_2} \end{array} \right\} \tag{7}$$

D. Experimental results:

Measurements were performed on a used cylindrical LIB: ICR14430-500 mAh; 3.7 V; SoH=97% using:

- PC-oscilloscope HANTEK/VOLTCRAFT-DSO-2250-100 MHz/2CH/250 MSa/s for measuring volt and current.
- PC-Data logger ISDS205B-24 MHz for recording.
- ELV-ALC8500-2Expert for charging/ discharging cycles.

Experimental measurements were made at different SoCs (10%, 30%, 50%, 70%, and 90%) and ambient temperatures (5°C, 20°C, 30°C, and 35°C). The model-parameters were conducted with the help of exponential function fitting (EFF).

The variations of the final identified parameters versus T are fitted by using the cubic polynomials in Matlab under discharge and charge conditions. Table 2 illustrate the experimental results.

TABLE II. EXPERIMENTAL RESULTS

Illustration of Experimental results					
Paramete r	SoC %	Temperature			
		5°C	20°C	30°C	35°C
R_c mΩ	10	132.72	114.48	108.41	106.38
	30	126.64	112.46	107.39	106.38
	50	119.55	110.43	103.34	101.31
	70	114.48	90.17	82.06	70.92
	90	110.43	87.13	79.02	67.88
R_d mΩ	10	150.96	120.56	111.44	108.41
	30	135.76	121.58	111.44	99.29
	50	131.71	119.55	109.42	91.18
	70	127.65	92.20	87.13	81.05
	90	123.60	89.16	84.09	80.04
R_{lc} mΩ	10	13.17	11.14	10.13	9.12
	30	16.21	14.18	13.17	11.14

	50	15.20	14.18	12.16	12.16
	70	17.22	15.20	12.16	10.13
	90	18.24	17.22	16.21	13.17
C_{1c} F	10	395.12	491.37	557.22	587.62
	30	506.57	612.95	699.06	729.46
	50	567.36	668.67	729.46	769.98
	70	496.44	577.49	688.93	729.46
	90	466.04	567.36	678.80	709.19
R_{2c} m Ω	10	61.80	50.66	43.56	40.53
	30	55.72	45.59	39.51	36.47
	50	52.68	43.56	40.53	35.46
	70	50.66	44.58	35.46	33.43
	90	42.55	34.45	30.39	27.35
C_{2c} F	10	3697.9	3546.0	3495.3	3292.7
	30	4255.2	4001.9	4001.9	3748.6
	50	4863.0	4609.8	4559.1	4204.5
	70	4761.7	4457.8	4559.1	4153.8
	90	5369.6	4913.7	4863.0	4559.1
R_{1d} m Ω	10	22.29	22.29	20.26	17.22
	30	15.20	14.18	12.16	12.16
	50	13.17	12.16	12.16	11.14
	70	9.12	7.09	5.07	4.05
	90	10.13	9.12	9.12	8.11
C_{1d} F	10	293.81	359.66	420.45	501.50
	30	618.01	709.19	754.78	845.97
	50	567.36	688.93	764.92	815.57
	70	405.25	506.57	557.22	567.36
	90	506.57	592.68	628.14	648.41
R_{2d} m Ω	10	58.76	44.58	38.50	36.47
	30	57.75	46.60	39.51	37.49
	50	55.72	45.59	38.50	35.46
	70	46.60	40.53	33.43	32.42
	90	48.63	39.51	34.45	26.34
C_{2d} F	10	3394.0	3090.0	3951.2	2887.4
		0	6	2	3
	30	4761.7	4305.8	4255.1	4153.8
		3	2	6	5
	50	4964.3	4356.4	4305.8	4103.1
		6	8	2	9
	70	5470.9	4609.7	4559.1	4305.8
		2	6	0	2
	90	5977.4	4964.3	4863.0	4660.4
		9	6	4	2

E. Model validation:

The verification is done by comparing the experimental and simulation battery voltage under HPPC test profile at T=25°C, and SoC=70%. As shown in Fig. 4, observed voltage error of simulated values comparing to measured voltage was less than 0.019 V as mean absolute error (less than 0.61% as percentage error of simulated values). Through this model, as a result, we are able to determine with acceptable accuracy the relationship between the temperature and change of the internal parameters, which makes this model a good basis for the systems of measuring and analyzing the state and aging of lithium-ion batteries based on artificial intelligence techniques.

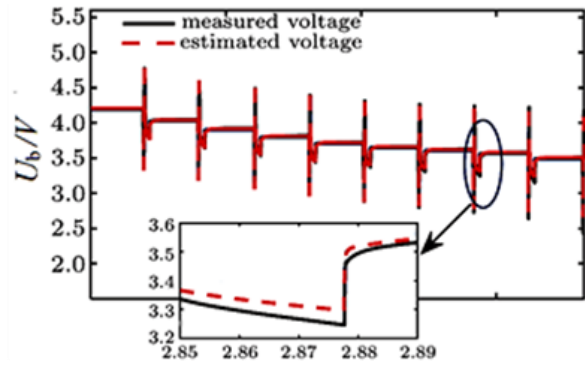


Fig. 4. Experimental and simulation battery voltage under HPPC test profile at T=25°C, and SoC=70%

IV. SOC ESTIMATION

A. Background:

State of charge is a very important indicator for assessing the status of the available energy capacity of batteries in ESS used in various applications. Especially when it comes to online battery monitoring and measurement.

However, the matter may differ when it is required to assess the state of the batteries offline, here SoC will only be very important with indirect estimation of battery aging state.

Therefore, the SoC estimate of LIBs has been extensively studied due to their fast charge, long life cycle, and high energy density properties. However, an accurate SoC assessment remains a challenge due to their varying characteristics under different working environments [13].

The state of charge is indicated digitally as the percentage of charge available in the battery. Where 100% indicating full capacity and 0% indicating that no more charge is left in the battery [1]. SoC refers normally to the available battery capacity that can be withdrawn from the battery and its estimation is very important to prevent its over-discharge or over-charge as well as to operate the battery in such a manner that aging effects are reduced [14].

A several different methods have been proposed to estimate SoC with varying degrees of accuracy and complexity for each of them.

Table 3 describes the most common methods with their main drawbacks [15][16].

TABLE III. OVERVIEW ON THE SOC ESTIMATION METHODS [15][16]

SoC Estimation Methods			
Method	Description	Advantages	Drawbacks
Coloumb Counting (CC)	Discrete integral of the input current.	Simple and intuitive approach.	It requires to know the initial SoC value.

		Low-cost sensors for current measurement	It is affected by error for current accumulation.
		Combination with other techniques is possible	It does not consider any physical property of the cell.
		Computationally efficient.	It requires accurate current measurements. It is not able to cope with partial charge/discharge cycles.
			It requires to know the actual capacity C_a .
Open Circuit Voltage (OCV)	Matching of the terminal voltage with the OCV-SoC lookup table.	It takes into account physical properties of the cell.	Internal resistance and charge redistribution phenomena weak the correlation between voltage and SoC.
		Combination with other techniques is possible	Flat SoC-OCV curves make the SoC prediction more sensible to measurement noises and errors
		Computationally efficient	
Model - Based	SoC estimated from the relationship between measured battery signals (voltage, current, and temperature) and SoC employing a battery model.	It studies the electrical behaviour of the battery	It requires to know the reference initial parameters of the battery which can only be parameterized accurately for new batteries in the laboratory.
		Usefull for on-line monitoring because of on-line measurement of model input signals	It requires high computing cabability.
		Combination with other techniques is possible	The accuracy of the estimation depends largely on climate variables.
Machine Learning	SoC estimated with a black-box function approximation tool	Combination with other techniques is possible to switch to grey-box function.	It requires a huge amount of historical data for training the tool.
		Usefull for on-line monitoring.	Collect the training data involves expensive testing equipment and long-lasting tests.
		High accuracy after good training and fine tuning.	The relationship between voltage, temperature, current, and SoC is hidden. It may require further data processing and filtering.
State Observe	It uses nonlinear KFs for estimating SoC as a state variable of the system.	Self correction method.	Can be computationally demanding.
		It can provide information about the	It requires an accurate model of electrochemical cells

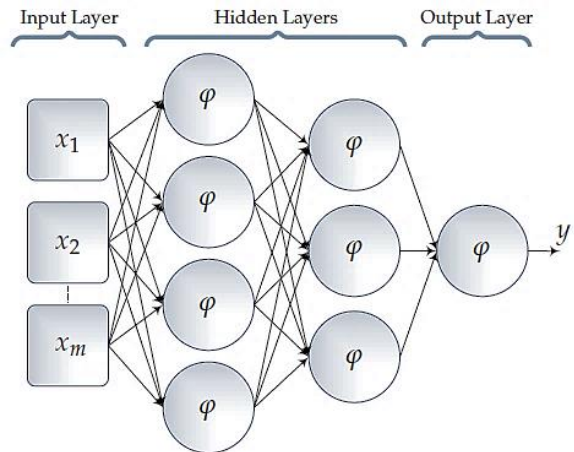
estimation accuracy

B. A theoretical introduction to artificial neural networks:

Artificial neural networks are machine learning technique, it is a powerful processing tool enclosing the ability of learning from experience. From a general point of view ANNs are a data-driven black box technique aiming at learning and modeling the input-output relationship of a given process from the knowledge of a set of input-output measurements only [17][18].

Similar to other machine learning algorithms, neural networks are also natural inspired techniques. In particular, ANNs aim to emulate the functionality and learning ability of the animal brain. They are therefore organized as a network of atomic computing units called artificial neurons. Each of these units processes its inputs very simply and forwards the resulting output to the other neurons [15].

Several different structures of ANNs have been developed but the feed-forward neural networks are the basic architecture of ANNs and the most suitable example is the Multi-Layer Perceptron (MLP) shown



in Fig. 5 [15].

Fig. 5. Architecture of a feed-forward MLP [15]

Feed-forward MLPs usually consist of a succession of layers in which the output of each neuron is connected to the immediate following layer only. Therefore, the inputs (x_i) are processed and propagated in only one direction moving layer by layer to the output neuron (y). Equation (8) describes the relation between output and inputs [15].

$$y = \varphi(x_1w_1 + \dots + x_iw_i + \dots + x_mw_m + b) \tag{8}$$

where w_i is the related weight, b is a bias term, and φ is a nonlinear or linear transformation called activation

function, the most common activation functions are shown in Fig. 6.

Choosing the appropriate activation function depends on the characteristics of the input values and their relationship to the outputs [15][19].

From the above we can conclude that feed-forward neural networks are pure combinatory and memoryless processing tools because the current output depends only on the current input. In particular, MLPs are characterized by fully connected layers, meaning that each neuron receives as input the output of all the neurons composing the previous layer and it propagates its output to all the neurons of the following layer. The MLP architecture is organized in three groups: the input layer, one or more hidden layers, and the output layer. In particular, the input layer is not composed of real neurons, but it aims only at feeding the first hidden layer with the overall inputs of the network [15].

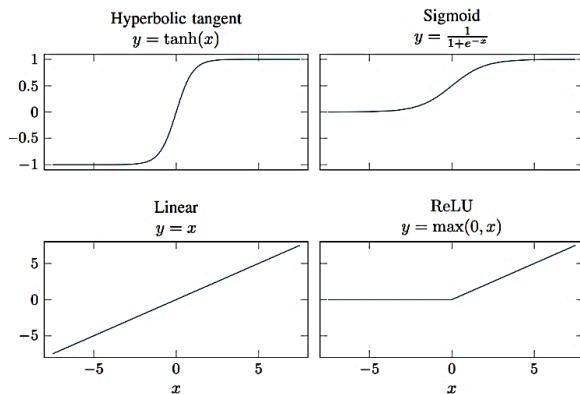


Fig. 6. The most common activation functions [15]

The weights w_i are determined during the training phase of the neural network. Thus, training ANNs is the most critical phase that determines how those ANNs are accurate [20].

The weights are calculated during the training phase by minimizing the loss function (usually a quadratic function of the output error), one common technique that is widely used in training ANNs is the back-propagation, which is a supervised learning method that is commonly used in the training phase in order to calculate the weights. Back-propagation uses a steepest-descent technique based on the computation of the gradient of the loss function with respect to the network parameters [20].

After the input and target for training data is created, next step is to divide the data up into training, validation and test subsets. In the case of 100 samples for training, (70%) of data are used for the training and 21 samples (15%) of each data for validation and testing. Table 4 shows the numbers of samples for training, validation and test data [19].

TABLE IV. THE NUMBER OF SAMPLES FOR TRAINING, VALIDATION AND TEST SET [19]

Data Types	Number of Samples
Training	100
Validation	21
Testing	21

Neural networks are sensitive to the number of the hidden layers and their neurons. Too few neurons in the hidden layer prevent it from correctly matching inputs to outputs. On the other hand, too many may impede generalization and increasing training time. Therefore the number of hidden layers and their neurons is selected through experimentation to find the optimum number of neurons for a predefined minimum of mean square error in each training process [19].

C. SoC-Estimation using neural networks:

These methods are often referred to as the black box functional approximation tools. Which is seen as a disadvantage of these methods as the relationship between voltage, temperature, current and SoC is hidden.

In order to get away from the disadvantages of adopting this method on the black-box principle, we have in our research relied on the electrochemical dynamic response of ECM-parameters which affected directly by SoC as inputs to the neural network.

Several attempts have been developed to estimate SoC using measuring of internal resistance, and the results have been mixed. Additives affect strongly Internal Resistance and make its behaviour very complex, making ohmic test unreliable for SoC estimation [21]. The electrochemical dynamic response gives a clearer perception of the change in the characteristics of the battery with the change in its state of charge. To illustrate the idea, two short brief load pulses are applied, the response time on attack and recovery is measured. As seen in Fig. 7, a battery with SoC=100% resists the attack and recovers quickly whereas the impact of a battery with SoC=70% is larger and the recovery is slower [21].

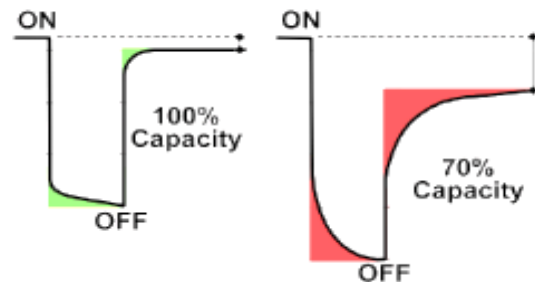


Fig. 7. Electrochemical dynamic response [21]

The same is also the case when charging pulses are applied, since due to the variation in the acceptability of the charge when the state of charge is different, this also causes variations in the shape and amount of voltage drop and time constants in recovery and relaxation period.

The non-linear variation of the internal resistance of the battery versus SoC leads to nonlinearity in the relationship between the SoC and the time constant and the voltage drop in the electrochemical dynamic response curve. This is a main reason that makes artificial neural networks a suitable solution to this issue, as the neural networks are distinguished by their ability to deal with these complex dynamic variations. According to Fig. 7, which illustrates the concept of our method, the voltage drops due to ohmic resistance by applying the charge and discharge pulses, as well as the time constants in the recovery and relaxation period after these pulses, will be considered with temperature as inputs of the neural network.

Since the ECM is employed to characterize the physical processes occurring in the battery, the ohmic resistance $R_{c,d}$ is related to the electrolyte and connection resistance, the RC network ($R_{1,2}/C_{1,2}$) represents the effect of the activation polarization (charge-transfer and double-layer). In general, the majority of the concentration polarization processes have larger time constants ($\tau_{2c,d}$) compared to time constants of the activation polarization processes ($\tau_{1c,d}$) [22][23].

The detailed architecture of the ECM with the second-order RC network is shown in Fig. 8, it shows all SoC relevant parameters ($\Delta U_{c,d}$; $\tau_{1c,d}$; $\tau_{2c,d}$) connected to the corresponding RC network ($R_{1,2}/C_{1,2}$) [22][23].

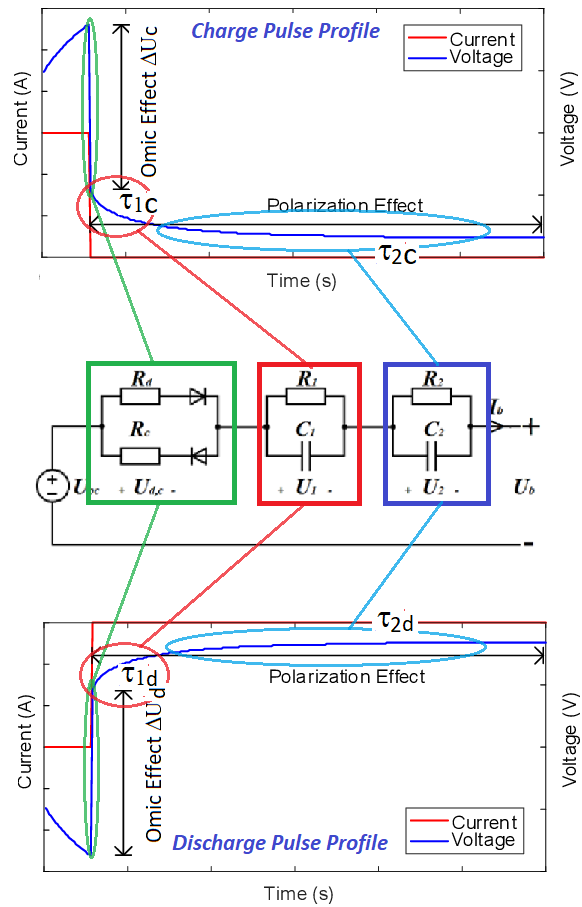


Fig. 8. Architecture of the ECM with SoC relevant parameters connected to the corresponding RC network

With this, we have completed the final visualization of the inputs of the neural network: T , $|I_b|$, ΔU_c , ΔU_d , τ_{1c} , τ_{1d} , τ_{2c} , τ_{2d}

The developed feed-forward MLP neural network in this paper for SoC estimation with back-propagation training, shown in Fig. 9, consists of input layer with eight inputs, one hidden layer with 35 neurons (obtained experimentally), and output layer with one output (SoC).

The linear activation function is used in the output layer, and the sigmoid activation function in the hidden layer.

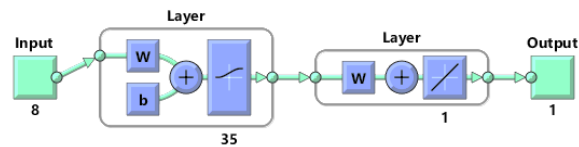


Fig. 9. Architecture of SoC neural network

In the next section, we will present the experimental results and the results of the neural network training

process, and we will discuss the final results of estimating SoC.

D. Neural network training and SoC-estimation results:

From the HPPC test of charging and discharging pulses applied in section of battery modelling, shown in Fig. 3 (period of charge/discharge pulses is 10 sec and relaxation period is 40 sec), we obtained $\tau_{1c}-\tau_{1d}-\tau_{2c}-\tau_{2d}$ from (6) by applying exponential fitting function.

I_b is $-0.5C= -250mA$ during charge pulse and $0.5C= 250mA$ during discharge pulse.

$\Delta U_c, \Delta U_d$ are obtained as:

$$\Delta U_c = R_c * I_b \tag{9}$$

$$\Delta U_d = R_d * I_b \tag{10}$$

Table 5 illustrate the experimental results for training ANN.

TABLE V. EXPERIMENTAL RESULTS OF SoC ESTIMATION ANN

Illustration of Experimental results					
Parameter	SoC%	Temperature			
		5°C	20°C	30°C	35°C
τ_{1c} sec	10	5.20	5.48	5.65	5.36
	30	8.21	8.69	9.21	8.13
	50	8.62	9.48	8.87	9.36
	70	8.55	8.78	8.38	7.39
	90	8.50	9.77	11.00	9.34
τ_{1d} sec	10	6.55	8.02	8.52	8.64
	30	9.39	10.06	9.18	10.28
	50	7.47	8.38	9.30	9.09
	70	3.70	3.59	2.82	2.30
	90	5.13	5.40	5.73	5.26
τ_{2c} sec	10	228.54	179.63	152.27	133.44
	30	237.11	182.45	158.12	136.72
	50	256.20	200.82	184.76	149.09
	70	241.21	198.72	161.66	138.88
	90	228.49	169.26	147.81	124.71
τ_{2d} sec	10	199.44	137.75	152.12	105.31
	30	274.98	200.67	168.13	155.71
	50	276.63	198.62	165.77	145.50
	70	254.97	186.81	152.43	139.60
	90	290.69	196.15	167.52	122.76
ΔU_c mV	10	33.18	28.62	27.10	26.59
	30	31.66	28.11	26.85	26.59
	50	29.89	27.61	25.83	25.33
	70	28.62	22.54	20.52	17.73
	90	27.61	21.78	19.76	16.97
ΔU_d mV	10	37.74	30.14	27.86	27.10
	30	33.94	30.39	27.86	24.82
	50	32.93	29.89	27.35	22.80
	70	31.91	23.05	21.78	20.26
	90	30.90	22.29	21.02	20.01

As a result of training the SoC-ANN, table 6 presents the results and error and performance of the ANN.

TABLE VI. TRAINING OF SoC ANN RESULTS

Number of Layers	2
------------------	---

Number of Neurons in Hidden Layer	35
Length of Input Vector	8
Number of Training Vectors	20
The rate of Validation Vectors	3
The rate of Test Vectors	3
Length of Output Vector	1 (SoC)
Error MSE (e [^])	-18
Number of epochs	273

As shown in Table 6, the training process stopped after 273 epochs successfully after reaching the expected performance at an internal training error of rank e[^]-18 as MSE.

The performance of the neural network was verified by inserting two vectors at which the network was not trained.

The estimation of SoC, as shown in Table 7, was with acceptable accuracy performed, as the maximum prediction error was 1.89%.

TABLE VII. THE VERIFICATION OF SoC ANN-PERFORMANCE

Actual SoC%	60	95
Estimated SoC% (ANN Output)	59.1	96.8
Estimation Error	1.52%	1.89%

V. SoH ESTIMATION

A. Background:

The battery state of health and capacity decrease after a battery is repeatedly charged and discharged, because of the output power of battery is affected as a function to number of cycles, which results in performance degradation [24][25].

For second life batteries operation, accurate prediction of the efficient performance and SoH of batteries is very critical, because of the wrong selecting leads to ineffective performance and storage system failure, here SoH estimation is very important as the batteries performance should be identified to ensure the capability of serving in any condition. And since LIBs can still be used in many applications after removal from their first use in electric vehicles, e.g. as a storage media in photovoltaic systems and for grid support. Therefore, there is a great need to develop a reliable methodologies to characterize the expected performance of LIBs after their first life in Evs [24].

Figure 10 shows a summary of the life cycle of lithium-ion batteries. In early life in EVs the batteries are consumed up to a state of health in the range of 70-80%, at which the use of batteries in EVs becomes practically ineffective. In theory, the batteries could then be

transported for service in second life in many applications such as stationary storage systems. But that depends on the state of health of the batteries, as they must be at least 40% in order for their investment in the second life to be feasible from a practical and economic point of view. Otherwise, the batteries must be recycled [25][26].

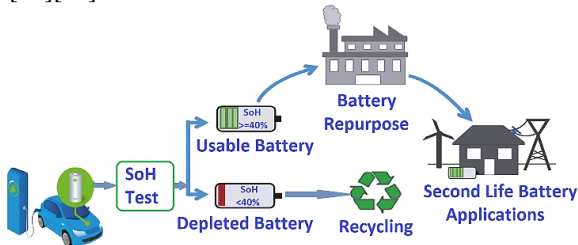


Fig. 10. The life cycle of lithium-ion batteries used in EVs

Several methods in the previous researches are discussed and implemented different techniques for the SoH estimation with varying degrees of accuracy and complexity for each of them.

Table 8 describes the most common methods with their main drawbacks [15][16].

TABLE VIII. OVERVIEW ON THE SoH ESTIMATION METHODS [15][16]

SoH Estimation Methods			
Method	Description	Advantages	Drawbacks
Capacity Test	Direct measurement of Cn by performing a controlled charge/discharge test.	Simple and intuitive approach.	Offline procedure. It requires expensive testing equipment.
		Computationally efficient.	It is necessary to disassemble the ESS.
			It is affected by error accumulation.
Internal Resistance Measurement	Direct measurement of the internal resistance by applying a short current pulse to the cell.	It takes into account physical properties of the cell.	Offline procedure. It requires expensive testing equipment.
		A simple theory of approach.	It is necessary to disassemble the ESS.
Electrochemical Impedance Spectroscopy (EIS)	Retrieving a SoH index from the analysis of the Nyquist diagram of Z(w).	Online procedure.	EIS hardware is very expensive and voluminous.
		It takes into account physical properties of the cell.	It cannot be applied to numerous electrochemical cells.
Machine Learning	SoH estimated with a black-box function approximation tool.	Online procedure. Acceptable accuracy after good training and fine tuning.	It requires a huge amount of historical training data. Collect the training data involves expensive testing equipment and long time.

		It may require further data processing and filtering.
State Observe	Use of a dual nonlinear KF for estimating Cn	Self correction method. It can provide information about the estimation accuracy
		Can be computationally demanding.
		It requires an accurate model of electrochemical cells
		It needs very accurate SoC estimations

B. SoH-Estimation using neural networks:

In contrast to the SoC, there is no defined and clarified relationship between SoH and electrical operating parameters, such as I_b and U_b . Therefore, new parameters for characterizing and defining SoH must be looked for.

Several properties of battery change with aging, such as Loss of Lithium Inventory (LLI), processes that make the lithium unusable for cycling, Loss of Active Materials (LAM), reduced amount of material enabling the lithium transfer, and structural damage to the components of the battery. The aging of the battery might depend on how it is used, referred to as cycle aging, or it may degrade without being used, referred to as calendar aging [27]. That means, the chemical structure of the battery will be affected primarily by the effect of aging, and this naturally leads to thinking about the internal impedance of the battery to try to find parameters to monitor SoH [28].

In this paper we will use the battery internal resistance, represented by the parameters of ECM which derived in section 3, taking into consideration the effect of SoC to monitor SoH, temperature will not be tacked into account because it was considered while estimating SoC and ECM parameters and both of them will be an input to estimate SoH.

SoH can be estimated by simple statistic methods, such as direct capacity test, but this type of methods will cost much time to obtain SoH as experimental result. As previously mentioned, ANNs considered an effective solution for handling with the behaviour of non-linear systems, cross-interaction between system variables and existing patterns in the data used to train the network [28][29].

In this paper we will use a feed-forward MLP neural network for SoH estimation.

The researcher Raghavendra Arunachala in [30] presented experimental study of LIBs aging with in details results of cycle aging of 8 Ah cell inclusive all parameters of second order ECM in case of discharge und from cycle zero until the cycle 1600. In this paper, the ANN will be trained using these results and we will refer to SoH as a cycle number not as a percentage rate as in the original reference. By the cycle 1600, the cell reaches to about SoH=70% as percentage rate.

Table 9 presents the experimental aging results as obtained in the previous study [30].

The inputs of the neural network will be then: R0, R1, R2, C1, C2, and SoC. The architecture of this network is shown in Fig. 11.

The back-propagation will be used as training method, the network consists of input layer with six inputs, one hidden layer with 30 neurons (obtained experimentally), and output layer with one output (SoH).

The linear activation function is used in the output layer, and the sigmoid activation function for the hidden layer.

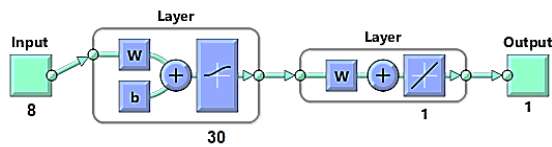


Fig. 11. Architecture of SoH neural network

TABLE IX. EXPERIMENTAL RESULTS [30]

SoC%	Cycle#	R0 mΩ	R1 mΩ	C1 F	R2 mΩ	C2 F
0	0	6.599	1.922	2379	3.45	2319
	500	7.96	2.273	2041	3.606	2227
	800	9.328	3.054	1660	3.745	2071
	1200	14.389	3.239	1568	3.775	2035
	1600	20.051	4.074	4002	4.073	2248
10	0	7.086	1.726	4468	3.377	1889
	500	8.556	2.243	3156	3.41	1781
	800	9.736	3.099	1987	3.556	1677
	1200	14.711	3.355	1721	3.614	1698
	1600	20.131	4.288	4179	3.867	1906
20	0	7.131	1.647	5371	3.369	1860
	500	8.697	2.385	2980	3.322	1707
	800	9.834	3.141	2029	3.423	1609
	1200	14.856	3.485	1679	3.476	1608
	1600	20.187	4.413	4159	3.668	1846
30	0	7.041	1.729	4170	3.132	2082
	500	8.711	2.567	2412	2.984	1937
	800	9.78	3.298	1710	3.022	1846
	1200	14.748	3.433	1534	3.089	1919
	1600	20.294	4.326	3836	3.444	2002
40	0	6.565	1.923	1908	3.83	1923
	500	8.409	2.861	1423	3.527	1919
	800	9.576	3.439	1317	3.52	1872
	1200	14.831	3.828	1254	3.553	1827
	1600	20.095	4.676	3471	3.852	1895
50	0	6.596	2.003	1967	4.059	1920
	500	8.477	3.106	1413	3.661	1959
	800	9.754	3.926	1274	3.613	1851
	1200	14.955	4.289	1228	3.614	1814
	1600	19.829	5.424	2986	3.954	1911
60	0	6.672	2.113	2006	4.393	1864
	500	8.526	3.386	1410	3.927	1885
	800	9.905	4.338	1285	3.848	1752

70	1200	15.052	4.756	1219	3.791	1729
	1600	19.928	5.848	2839	4.023	1846
	0	6.783	2.499	1844	4.714	1719
	500	9.046	4.41	1874	5.348	1154
	800	10.493	5.557	1697	6.224	9526
80	1200	15.511	5.727	1512	7.049	9561
	1600	20.017	6.87	2617	7.307	1287
	0	6.9	2.787	1863	4.275	1659
	500	9.249	5.594	1694	4.657	1213
	800	10.752	7.382	1552	5.267	1013
90	1200	16.1	8.597	1549	5.732	8975
	1600	19.56	12.071	1799	6.442	9284
	0	7.114	3.686	1732	7.695	1073
	500	9.548	6.128	1835	7.78	8676
	800	11.107	7.926	1689	8.361	8005
100	1200	16.403	9.118	1652	8.187	7879
	1600	19.686	12.778	1918	8.169	9284
	0	10.081	8.026	4253	51.164	3545
	500	11.841	9.391	3443	32.254	4092
	800	13.134	10.099	2915	22.752	3899
1200	18.134	11.231	2518	20.034	4015	
1600	19.675	15.824	1880	17.901	4637	

As a result of training the SoH-ANN, table 10 presents the results and error and performance of the ANN.

TABLE X. TRAINING OF SoH ANN RESULTS

Number of Layers	2
Number of Neurons in Hidden Layer	30
Length of Input Vector	6
Number of Training Vectors	50
The rate of Validation Vectors	7
The rate of Test Vectors	7
Length of Output Vector	1 (SoH)
Error MSE (e [^])	-24
Number of epochs	198

As shown in Table 10, the training process stopped after 198 epochs successfully after reaching the expected performance at an internal training error of rank e^{^-24} as MSE.

The performance of the neural network was verified by inserting five vectors at which the network was not trained.

The estimation of SoH, as shown in Table 11, was with acceptable accuracy performed, as the maximum prediction error was 2.8%.

TABLE XI. THE VERIFICATION OF SoH ANN-PERFORMANCE

<i>Actual Cycle#</i>	<i>800</i>	<i>500</i>	<i>800</i>	<i>1200</i>	<i>1600</i>
<i>@ SoC</i>	<i>10</i>	<i>50</i>	<i>90</i>	<i>70</i>	<i>30</i>
Estimated Cycle# (ANN Output)	806	514	793	1213	1583
Estimation Error	0.75%	2.8%	0.87%	1.08%	1.06%

VI. CONCLUSION AND FUTURE WORK

A. Conclusion:

This paper presents a robust, fast, and non-destructive measurement procedure to estimate the state of charge and state of health of Li-ion batteries using one of artificial intelligent tools, artificial neural networks, to overcome the obstacles of very long testing time in traditional methods and to obtain a good level of accuracy suitable for this kind of applications.

From the results of the research, the following can be concluded:

- Several methods which used ANNs in SoC estimation have depended on the online measurement of current and voltage as inputs of ANN, so they referred to as the black box functional approximation tools, because the relationship between voltage, current and SoC is hidden. In the method presented in this paper this disadvantage was overcome relied on the electrochemical dynamic response parameters (voltage drops and time constants) which affected directly by SoC as inputs to the neural network.
- The same applies also to the state of health, the battery internal resistance represented by the parameters of ECM are used as neural network inputs for SoH estimation because of the chemical structure of the battery will be affected primarily by the effect of aging.
- Because temperature has a high degree of influence on the behavior and performance of battery systems, it was taken into account during the derivation of the ECM parameters, as well as during the estimation of the SoC, which in its entirety were taken into account to estimate the SoH.
- The developed idea and methodology have been applied experimentally on a specific type and specific capacity of batteries. As we have seen through the results in the previous paragraphs a very good results have been obtained for this type and capacity. However,

the challenge remains in generalizing this model and developing the structure of the neural networks used in terms of adding new inputs to reach a flexible methodology capable to deal with different types of batteries and with different nominal capacities within a specified range. Of course, this requires additional inputs to the neural networks to indicate the type used, as well as the suitability of the network in terms of activation functions, the number of hidden layers and possibly the type of networks used.

B. Future work:

- The training data used in the SoH neural network was only taken for the discharging status. Additionally, experiments and measurements have yet to be done for the charge status to obtain a larger number of training data in order to obtain better accuracy as well as developing the neural network for possible error correction by comparing the SoHs values resulting from the charging and discharging status.
- A lot of experiments and measurements must be made, as well as researching ways to develop neural network structures in order to try to generalize the system to include a wide range of types of battery cells with different capacities. Also, it may be necessary to add the HPPC-pulse amplitude control feature to fit the nominal capacity of the tested battery cell automatically.
- Developing the HPPC test of the SoC neural network by adding other consecutive pulses at specific intervals and varying amplitudes in order to obtain consecutive SoCs values with a time delay and a specific charge difference in order to provide the neural network with the self-calibration feature.

REFERENCES

- [1] X. Theron, and T. Yilo, "The integration of second life EV battery and vehicle-to-grid charging into a micro-grid environment" e-Mobility Technology Innovation Programme, Nelson Mandela University, Port Elizabeth, 6031, South Africa.
- [2] J. Mathews, B. Xu, W. He, V. Barreto, T. Buonassisi, and et al., "Techno-economic model of a second-life energy storage system for utility-scale solar power considering li-ion calendar and cycle aging", European Union's Horizon 2020 research and innovation programme.
- [3] M. Najeeb, and U. Schwalbe, "Developing an advanced equivalent circuit model for LIBs for battery monitoring purpose" IEEE, in press.
- [4] F. Saidani, F. X. Hutter, R. G. Scurtu, W. Braunwarth, and J. N. Burghartz, "Lithium-ion battery models: a comparative study and a model-based powerline communication", Adv. Radio Sci., vol. 15, pp. 83–91, 2017.

- [5] S. G. Beechu, "Development of lithium ion battery dynamic model", Technische universitaet chemnitz., Master thesis, 331230, 2015.
- [6] Q. Navid, and A. Hassan, "An Accurate and Precise Grey Box Model of a Low-Power Lithium-Ion Battery and Capacitor/Supercapacitor for Accurate Estimation of State-of-Charge", *MDPI-Batteries* 2019, 5, 50; doi:10.3390/batteries5030050
- [7] C. Zhang, K. Li, S. Mcloone, and Z. Yang, "Battery modelling methods for electric vehicles - a review", *IEEE, European Control Conference*, 2014, doi: 10.1109/ECC.2014.6862541.
- [8] T. R. B. Grandjean, A. McGordon, and P. A. Jennings, "Structural identifiability of equivalent circuit models for li-ion batteries", *MDPI-Energies*, 2017, 10, 90; doi:10.3390/en10010090.
- [9] H. Li, X. Wang, A. Saini, Y. Zhu, Ya-Ping Wang, "State of charge estimation for lithium-ion battery models based on a thermoelectric coupling model", *Int. J. Electrochem. Sci.* 15, 3807 – 3824, 2020, doi: 10.20964/2020.05.41.
- [10] L. Zhang, S. Wang, Daniel-I. Stroe, C. Zou, C. Fernandez, and et al., "An accurate time constant parameter determination method for the varying condition equivalent circuit model of lithium batteries", *Energies* 13, 2057, 2020, doi: 10.3390/en13082057.
- [11] Hans-G. Schweiger, O. Obeidi, O. Komesker, A. Raschke, M. Schiemann, and et al., "Comparison of several methods for determining the internal resistance of lithium ion cells", *MDPI-Sensors* 10, 5604-5625, 2010, doi: 10.3390/s100605604.
- [12] J. Su, M. Lin, S. Wang, J. Li, J. Coffie-Ken, and et al., "An equivalent circuit model analysis for the lithium-ion battery pack in pure electric vehicles", *Measurement and Control* 52(3-4), 193-201, 2019, doi: 10.1177/0020294019827338.
- [13] M. A. Hannan, M. S. H. Lipu, A. Hussain, P. J. Ker, T. M. I. Mahlia, and et al., "Toward enhanced state of charge estimation of lithium-ion batteries using optimized machine learning techniques", *Scientific Reports*, 2020, 10:4687, doi: 10.1038/s41598-020-61464-7.
- [14] J. P. R. Barrera, N. M. Galeano, and H. O. S. Maldonado, "SoC estimation for lithium-ion batteries: review and future challenges", *MDPI- Electronics* 2017, 6, 102, doi: 10.3390/electronics6040102.
- [15] M. Luzi, "Design and implementation of machine learning techniques for modeling and managing battery energy storage systems", University of Rome-La Sapienza, Ph.D. Thesis, February 2019.
- [16] W. Waag, C. Fleischer, and D. U. Sauer, "Critical review of the methods for monitoring of lithium-ion batteries in electric and hybrid vehicles", *Journal of Power Sources*, 258 (2014) 321-339.
- [17] G. P. Zhang, "Neural networks for classification: a survey", *IEEE Transactions On Systems, Man, And Cybernetics, Part C: Applications And Reviews*, VOL. 30, NO. 4, pp. 451-462, November 2000.
- [18] A. Krizhevsky, I. Sutskever, and G. E. Hinton, "ImageNet classification with deep convolutional neural networks", *Communications of the ACM*, VOL. 60, NO. 6, pp. 84-90, June 2017.
- [19] K. Suzuki, "Artificial neural networks - industrial and control engineering applications", *InTech Janeza Trdine* 9, 51000 Rijeka, Croatia, March 2011.
- [20] A. A. Hussein, "Kalman Filters versus Neural Networks in Battery State - of - Charge Estimation: A Comparative Study", *SciRes, International Journal of Modern Nonlinear Theory and Application*, 3, pp. 199 - 209, December 2014.
- [21] "Testing Lithium-based Batteries", Battery University, BU-907, (<http://batteryuniversity.com/>).
- [22] Q. Yang, J. Xu, B. Cao, and X. Li, "A simplified fractional order impedance model and parameter identification method for lithium-ion batteries", *Plos One*, doi:10.1371/journal.pone.0172424 February 17, 2017.
- [23] J. Yang, W. Huang, B. Xia, and C. Mi, "The improved open-circuit voltage characterization test using active polarization voltage reduction method", *Applied Energy* 237 (2019), pp. 682–694, January 2019, doi: 10.1016/j.apenergy.2019.01.060.
- [24] N. Khan, F. U. M. Ullah, Afnan, A. Ullah, M. Y. Lee, and et al., "Batteries state of health estimation via efficient neural networks with multiple channel charging profiles", *IEEE Access*, Vol. xx2017, doi: 10.1109/ACCESS.2020.3047732, IEEE Access.
- [25] E. M. Laserna, E. S. Zabala, I. V. Sarria, D. I. Store, M. Swierczynski, and et al., "Technical viability of battery second life: a study from the ageing perspective", *IEEE Transactions on industry applications*, Vol. 54, NO. 3, pp. 2703-2713, May/June 2018.
- [26] E. Locorotondo, V. Cultrera, L. Pugi, L. Berzi, M. Pasquali, and et al., "Electrical lithium battery performance model for second life applications", *European Union's Horizon* 2020.
- [27] H. Johnsson, "A Neural Network Approach to Absolute State-of-Health Estimation in Electric Vehicles", Chalmers University Of Technology, Gothenburg, Sweden, Master thesis, 2018.
- [28] D. Yang, Y. Wang, R. Pan, R. Chen, and Z. Chen, "A neural network based state-of-health estimation of lithium-ion battery in electric vehicles", *ScienceDirect, Energy Procedia* 105, pp. 2059 – 2064, 2017, doi: 10.1016/j.egypro.2017.03.583.
- [29] A. Rastegarpanah, J. Hathaway, M. Ahmeid, S. Lambert, A. Walton, and et al., "A rapid neural network-based state of health estimation scheme for screening of end of life electric vehicle batteries", *J Systems and Control Engineering* 2021, Vol. 235(3), pp. 330–346, july 2020, doi: 10.1177/0959651820953254
- [30] R. Arunachala, "Influence of cell size on performance and lifetime of lithium-ion batteries", Technische Universitaet Muenchen, Ph.D. Thesis, November 2017.